



Published in final edited form as:

*J Biomed Nanotechnol.* 2015 March 1; 11(3): 447–456. doi:10.1166/jbn.2015.2038.

## Biom mineralization of Natural Collagenous Nanofibrous Membranes and Their Potential Use in Bone Tissue Engineering

Mingying Yang<sup>1,\*,\dagger</sup>, Guanshan Zhou<sup>1,\dagger</sup>, Harold Castano-Izquierdo<sup>2,\dagger</sup>, Ye Zhu<sup>2</sup>, and Chuanbin Mao<sup>2,\*</sup>

<sup>1</sup>Institute of Applied Bioresource Research, College of Animal Science, Zhejiang University, Yuhangtang Road 866, Hangzhou, Zhejiang 310058, China

<sup>2</sup>Department of Chemistry and Biochemistry, Stephenson Life Sciences Research Center, University of Oklahoma, 101 Stephenson Parkway, Norman, Oklahoma 73019-5300, United States

### Abstract

Small intestinal submucosa (SIS) membranes as a decellularized tissue are known to be a natural nanofibrous biomaterial mainly made of type I collagen fibers and containing some growth factors (fibroblast growth factor 2 and transforming growth factor  $\beta$ ) desired in tissue engineering. Here we show that the SIS membranes can promote the formation of bone mineral hydroxylapatite (HAP) crystals along the collagen fibers constituting the membranes from a HAP-supersaturated solution. The resultant biom mineralized HAP-SIS scaffolds were found to promote the attachment, growth and osteogenic differentiation of mesenchymal stem cells (MSCs) in both basal and osteogenic media by the evaluation of osteogenic marker formation. More importantly, the HAP-SIS scaffolds could induce the osteogenic differentiation in the basal media without osteogenic supplements due to the presence of HAP crystals in the scaffolds. Histological characterization of the MSC-seeded scaffolds showed that HAP-SIS scaffolds are biocompatible and promote the formation of new tissue *in vitro*. The biom mineralized SIS membranes mimic some aspects of natural bone in terms of the composition and nanostructures and can find potential use in bone tissue engineering.

### Keywords

Biom mineralization; Hydroxyapatite; Stem Cells; Tissue Engineering; Collagen

## INTRODUCTION

Bone defects caused by bone fractures and diseases such as osteoporosis, osteogenesis imperfecta, and massive bone loss due to trauma or cancer require enhanced bone formation for treatment, and have been major public health threats. Current treatments of bone defects use autologous bone grafts (bone taken from another part of the patient's own body),

autogenous bone grafts (bone taken from somebody else's body) or synthetic implants (e.g., metals and ceramics). However, they all have limitations.<sup>1,2</sup> Autologous bone grafts are restricted by the limited amount of the autograft as well as the donor site morbidity. Allograft bone may cause infections, immune rejection, and pathogen transmission from donor to host. The synthetic materials, once implanted, need revisions after a certain time. For instance, implants do not effectively interact with cells from native bone tissue, resulting in a layer of fibrous tissue in between the implant and native tissue. Therefore, tissue engineering is an alternative promising approach.<sup>3-9</sup> Instead of just implanting a new material into the body, it aims to use a scaffold to support cell growth and extracellular matrix (ECM) deposition to regenerate a fresh bone tissue. During bone development, cells grow, proliferate and differentiate within ECM, which is a natural scaffold mainly made of hydroxyapatite (HAP) crystals and collagen fibers. Therefore, to impart the biological properties of bone to tissue engineering scaffolds, a new process should be developed to fabricate ECM-mimicking biomaterials.

Although bone is a very complex tissue, the building block of its ECM is the HAP-decorated collagen fibers.<sup>10</sup> The HAP crystals in bones are formed as a result of biomineralization, which is a process by which minerals are nucleated and assembled in an organized manner under the control of collagen fibers in ECM.<sup>11,12</sup> In bone biomineralization, HAP crystals are nucleated and assembled within the collagen fibers, which are further hierarchically assembled into ECM.<sup>2,10,11,13</sup> To date, it is difficult to duplicate the elegance of the HAP nucleation and protein assembly in bone and the intricate composite nanoarchitectures of bone. In the field of bone tissue engineering, there is no report on the development of a scaffolding material that structurally, compositionally, and functionally mimics the real ECM in bone.

To mimic the composition of bone ECM to build a scaffold, we proposed to use a biomaterial derived from a decellularized natural tissue, small intestinal submucosa (SIS) membrane from pig, to form a mineralized HAP-SIS scaffold. SIS membrane is an acellular ECM material extracted from the small intestine of pigs.<sup>14</sup> After the cellular part is removed from the SIS membranes, the remnant is mainly composed of type I collagen fibers, glycoproteins, proteoglycans and some growth factors such as fibroblast growth factor 2 (FGF-2) and transforming growth factor  $\beta$  (TGF- $\beta$ ).<sup>15</sup> SIS membranes have been used as a biomaterial for regeneration, replacement or augmentation of lost tissues under experimental conditions. For instance, SIS membranes have been used in repairing several tissues including bladder,<sup>16-19</sup> abdominal wall,<sup>20-22</sup> intestine,<sup>23</sup> tendons and ligaments,<sup>24,25</sup> meniscus,<sup>26</sup> and blood vessels.<sup>27-29</sup> After implantation, the SIS membranes are remodeled by invasion of host's cells and blood vessel formation, allowing them to resemble native tissue.<sup>15</sup> SIS membranes have supported the growth of a variety of cells as pure cultures or in co-cultures.<sup>14</sup> In addition, SIS membranes have good mechanical properties.<sup>30</sup> These properties confer SIS membranes unique qualities as a bio-material suitable for tissue engineering. However, to the best of our knowledge, it has not been used to regenerate bone tissue. As a first step to apply SIS membranes to bone regeneration, in this work we studied the HAP nucleation on SIS membranes in order to form HAP-SIS scaffolds mimicking the composition of the bone ECM (Fig. 1) and tested the attachment, growth and osteogenic

differentiation of mesenchymal stem cells (MSCs) on biomineralized SIS membranes in both basal (without osteogenic supplements) and osteogenic (with osteogenic supplements) media (Fig. 2). We proposed the study of biomineralization of the SIS membranes not only because biomineralization of SIS membranes will make the resultant scaffolds mimic the composition of bone ECM but also because it has been shown that the presence of bone minerals in the scaffolds can promote the osteogenic differentiation of MSCs.<sup>31–35</sup> Therefore, we hypothesize that biomineralized SIS membranes will be better bone tissue engineering scaffolds than the pure SIS membranes.

## MATERIALS AND METHODS

### Nucleation of HAP on the SIS Membranes from HAP-Supersaturated Solution

The mineralization solution was a HAP-supersaturated solution prepared by using the method described by Silver-stone et al.<sup>36</sup> Briefly, a stock solution was firstly prepared to have an equivalent of 50 mM of calcium ions. The HAP powder (Sigma Aldrich) was dissolved in a solution of ddH<sub>2</sub>O containing 100 mM of hydrochloric acid and stirred until the powder was dissolved. 40 ml of the stock solution was poured into a plastic container and diluted to reach a volume of 450 ml with ddH<sub>2</sub>O. A solution of 0.05 M of potassium hydroxide was used to adjust the pH value of the solution to 7.0. Sodium chloride was added to the solution to reach a final concentration of 200 mM and then the final volume was adjusted to 500 ml with ddH<sub>2</sub>O. The solution was then sterilized through filtration by using a 0.2  $\mu$ m filter. The solution prepared by this method is the HAP-supersaturated solution<sup>36</sup> used in this work. We have successfully used this solution as a mineralization solution for studying the nucleation of HAP crystals on the biomimetic templates including functionalized titanium substrates,<sup>37–39</sup> filamentous bacteriophage,<sup>40,41</sup> bacterial flagella<sup>42</sup> and spider silk.<sup>43</sup> The SIS membranes (~ 1 cm wide and 6 mm thick) were bought from Sigma (vivoSIS<sup>®</sup>). To induce the biomimetic nucleation of HAP crystals on the SIS membranes, the SIS membranes were incubated in the HAP-supersaturated mineralization solution (Fig. 1). After different nucleation times (12, 24, and 96 h), the SIS membranes were taken out and washed with deionized water.

### Harvesting of Mesenchymal Stem Cells

MSCs were harvested from the femurs and tibias of Fisher 334 rat by the similar method described in our earlier work.<sup>44</sup> Briefly, the rats were first euthanized by CO<sub>2</sub> asphyxiation. Then femurs and tibias were retrieved and placed in falcon tubes containing Dulbecco's minimal essential media (DMEM) supplemented with 10% fetal bovine serum (FBS) (Atlanta Biologicals) and with 10,000 UI/ml penicillin G, 100 g/ml streptomycin sulfate and 25 g/ml amphotericin B (Sigma Aldrich). Subsequently, the falcon tubes were transferred to the laminar flow chamber, where under aseptic conditions the proximal epiphysis of the femur and distal epiphysis of the tibia were cut off. By inserting an 18 gauge needle mounted on a syringe loaded with DMEM in the distal epiphysis of the femur and proximal epiphysis of the tibia, the bone marrow was flushed through the opposite opening into another falcon tube. Then the chunks of marrow were destroyed by using the tip of a 5 ml serological pipette. The cell suspension was centrifuged at 450 g. After centrifugation, the supernatant was discarded and the pellet was re-suspended in 12 ml of

fresh media. 4 ml of the new suspension was deposited in three 75 ml flasks and a total volume of 11 ml was completed with fresh DMEM supplemented as above. The MSCs were cultured and expanded *in vitro* until 90% confluence was reached. The culture media were changed every other day.

### Cell Culture on Mineralized and Non-Mineralized SIS Membranes

A homemade device was fabricated to hold and manipulate the mineralized or non-mineralized SIS membranes for studying MSCs behaviors on the membranes (Fig. 2). Briefly, the bottoms of Eppendorf tubes were cut off. The SIS membranes were affixed in the frame created between the cap and the tube to stretch the membranes and avoid spill-over onto the tissue culture plate after MSCs seeding. A hole was made through the cap of the tube so that media and its nutrients could circulate and diffuse freely into the tube. The tubes were then placed upside down in the middle of 24-well plates (Biosciences) and the media were poured to cover them. The modified Eppendorf tubes were sterilized by autoclaving. SIS membrane manipulation and adaptation to the modified Eppendorf tube were carried out in the laminar flow chamber.

In order to seed MSCs on mineralized or non-mineralized SIS membranes, cells were first detached from the flasks using 0.25% trypsin-EDTA (Sigma-Aldrich). After 5 min, 5 ml of the fresh media were added to neutralize trypsin and the cell suspension was centrifuged at 400 g. The supernatant was then discarded and the cells were counted using a hemacytometer. Then the cell suspension was diluted to a concentration of 20,000 cells per half ml. Next, half ml of cell suspension was deposited on the SIS membranes (Fig. 2) and a volume of the same supplemented DMEM was added to each well.

### Experimental Group Design of MSCs Culture on Mineralized or Non-Mineralized SIS Membranes

The study on the attachment, proliferation and osteogenic differentiation of MSCs on the SIS membranes was divided into four main groups on the basis of the time of HAP nucleation (Table I): Group 1 is the group of cells seeded on the SIS membranes without HAP nucleation; Group 2 is the group of cells cultured on the SIS membranes with 12 h of HAP nucleation; Group 3 is the group of cells cultured on the SIS membranes nucleated for 24 h; and Group 4 is the group of cells seeded on the SIS membranes nucleated for 96 h. Each main group was divided into two subgroups (A or B) based on the type of media used to culture cells, i.e., Dulbecco's minimal essential media (DMEM) or osteogenic media (OST). Each SIS membrane was seeded with  $2 \times 10^4$  MSCs from the first passage. To evaluate the osteogenic capacity of the SIS-HAP scaffolds by themselves, cells were cultured in two types of media: DMEM and OST media that was supplemented with 50  $\mu\text{g}/\text{ml}$  of ascorbic acid (Sigma-Aldrich),  $10 \times 10^{-3}$  M Na- $\beta$ -glycerophosphate (Sigma-Aldrich) and  $1 \times 10^{-8}$  M dexamethasone (Sigma-Aldrich). The group of cells seeded on the non-mineralized SIS membranes was considered as a control group. For each group, cells were cultured for 5, 10 and 15 days. All experiments were conducted in triplicates.

### Scanning Electron Microscopy

Scanning electron microscopy (SEM) was used to study the morphologies of the crystals nucleated on the SIS membranes and the cells cultured on the SIS membranes. To prepare samples for imaging the crystals on the SIS membranes, after each mineralization time point (i.e., 0, 12, 24, and 96 h), the SIS membranes were taken out of the mineralization solution and rinsed with ddH<sub>2</sub>O before SEM characterization. To prepare samples for imaging the cells on the SIS membranes, the media was suctioned from the 24 well plates; the membranes were removed from the tubes and rinsed carefully three times with phosphate buffered saline (PBS); finally, they were fixed in 3.7% formaldehyde for 24 h. On the next day, the samples were moved to 70% ethanol until the day of processing for SEM. On the day of processing, the samples were cut and placed on the copper boats and dried. All of the samples were sputtered with AuPd in a Hummer<sup>®</sup> VI triode coater to enhance the conductivity. SEM images were observed with a Zeiss DSM-960A scanning electron microscope and imaged with the IXRF software.

### X-Ray Diffraction

After different mineralization times, the SIS membranes were removed from the mineralization solution, thoroughly rinsed with ddH<sub>2</sub>O to remove soluble salts and air dried. To evaluate the phase composition of the crystals nucleated on the SIS membranes, X-ray diffraction (XRD) was performed on a Scintag X2 diffractometer.

### DNA Assay to Quantify the Number of Cells on the SIS-HAP Scaffolds

The number of MSCs on the mineralized SIS membranes (SIS-HAP) after different times of culture (5, 10 and 15 days) was measured using the Picogreen dsDNA assay kit from Molecular Probes (Eugene, OR). The detailed protocol is available from the kit provider. This assay is based on the following principles: (1) The PicoGreen dye is essentially non-fluorescent and exhibits over 1000-fold fluorescent enhancement upon binding to cellular double-stranded (ds) DNA, resulting in an assay that displays a linear correlation between dsDNA concentration and fluorescence; (2) The assay is selective for dsDNA over RNA, oligonucleotides and single-stranded (ss) DNA; (3) The assay can be assembled in 96 well plates and quickly read on a spectrofluorometric microplate reader. The results were expressed as the number of cells per scaffold by using the DNA standard curve. The DNA extracted from a known number of cells was used to obtain the standard curve.

### Osteogenic Differentiation Assay

*In vitro* bone formation can be evaluated by examining the enzymatic activity of alkaline phosphatase (ALP), which is an early marker of osteogenesis and expressed by cells during bone formation.<sup>45,46</sup> ALP can modify a substrate (called *p*-nitrophenol phosphate) to produce a yellow product (called *p*-nitrophenol). The amount of this product reflects the amount of ALP formed during the osteogenic differentiation.<sup>47</sup> The ALP assay was performed by following our published protocol.<sup>44,48</sup> To further understand the osteogenic differentiation of MSCs at late stage, real-time polymerase chain reaction (PCR) analysis was used to profile the gene expression of a late-stage osteogenic differentiation marker, osteocalcin (OCN), by following our published protocol.<sup>44,49</sup>

## Histological Analysis of the MSC-Seeded HAP-SIS Membranes

After the constructs were removed from the Eppendorf tubes (Fig. 2) and rinsed with PBS for three times, they were fixed in 3.7% paraformaldehyde solution for 24 h. Then they were transferred to 70% ethanol and kept for 48 h before being processed for histology. On the day of the histological processing, all of the HAP-SIS membranes were dehydrated in graded series of ethanol, paraffin embedded and cut into sections with a thickness of 4  $\mu\text{m}$ . The sections were stained with hematoxylin and eosin (H & E) and imaged with a light microscope.

## Statistical Analysis

Statistical analysis was performed with the SPSS Statistics software. Multiple comparisons were performed using the Turkey HSD multiple comparison test. Statistical significance was considered at a confidence level of 95% ( $p < 0.05$ ). Quantitative data were shown as mean values  $\pm$  standard deviation.

# RESULTS

## Morphologies and Mineralization of SIS Membranes

XRD patterns show that pure SIS membranes did not contain any HAP crystals (Fig. 3). After nucleation for 12 h, HAP crystals were formed. More HAP crystals were formed at 24 h, as judged by the intensity of (211) peak. Surprisingly, at 96 h the intensity of (211) peak was reduced, suggesting the reduction of the amount of HAP crystals. It should be noted that no (001) peaks were found in the XRD patterns of all mineralized samples. This result indicates that probably HAP crystals were preferentially oriented with [001] direction parallel to the collagen fibers lying on the surface of the SIS membranes, which will cause (001) plane (perpendicular to the membrane surface) not to be diffracted by X-ray during XRD experiment (Fig. 3 inset). Under the SEM, the SIS membranes were composed of collagen fibers aligned and packed densely (Figs. 4(a) and (a')). At 12 h, the HAP crystals were found to be aligned along the collagen fibers (Figs. 4(b) and (b')). Due to the formation of more HAP crystals on the surface of the membranes, the individual HAP crystal-coated collagen fibers became not well resolved at 24 h (Figs. 4(c) and (c')). However, at 96 h, the individual HAP crystal-coated collagen fibers became well resolved again (Figs. 4(c) and (c')). It is likely that the HAP formation caused the mineralization solution to become unsaturated with respect to HAP at 96 h and thus HAP crystals not well attached to the surface of collagen fibers were dissolved again into the unsaturated solution. Consequently, only HAP-coated collagen fibers were visible under SEM. The SEM observation was consistent with XRD characterization, which shows a reduced amount of HAP crystals at 96 h (Fig. 3).

## Attachment of MSCs Onto Mineralized SIS Membranes

The SEM micrographs of cells seeded on HAP-SIS membranes after 15 days of *in vitro* culture showed that MSCs adhered to the HAP-SIS membranes and remained attached during the whole time of the study (Fig. 5). There was no major difference in cell adhesion between MSCs seeded in DMEM and OST media. However, the mineralized SIS scaffolds

appeared to favor the adhesion of MSCs onto the scaffolds when compared to the non-mineralized SIS scaffolds. In fact, it was reported that HAP as a natural bone component could promote the adhesion of MSCs to HAP-bearing scaffolds. For example, HAP favored the adhesion of MSCs to an HAP-coated poly (lactide-co-glycolide) (PLGA) scaffold in comparison to PLGA scaffold alone.<sup>31</sup> Thus it is not surprising to see that mineralized scaffolds tended to favor the adhesion of MSCs in our study. These results show that HAP-SIS membranes favor the adhesion of MSCs probably due to the presence of bone mineral, biocompatible collagen fibers and growth factors, which is consistent with the earlier reports that SIS membranes support the adhesion of other cell types.<sup>14</sup>

### **Proliferation of MSCs on Mineralized SIS Membranes**

The DNA content in a population of MSCs represents the number of MSCs on a scaffold,<sup>50</sup> and thus was used to quantify the proliferation of MSCs on the SIS-HAP membranes. Throughout the culture period, an increase in the cell number was observed on each group. This trend was maintained for both mineralized and non-mineralized SIS membranes (Fig. 6). The control group, Group 1A (i.e., cells seeded on non-mineralized SIS membranes), had the maximum rate of proliferation compared to groups 2B, 3A, 3B, 4A and 4B. The smallest cell proliferation was observed in Groups 4A and 4B, where cells were cultured on SIS membranes mineralized for 96 h in DMEM and OST media, respectively. An attenuated proliferation was observed for cells cultured on the biomineralized membranes as the mineralization time was increased compared to cells cultured on non-mineralized SIS membranes. This observation was visualized for cells cultured on mineralized SIS membranes in both DMEM and OST media. Cell proliferation between groups 2B, 3A and 3B looked very similar and showed no significant differences. Groups 4A and B had significantly fewer cells than the other groups. However, those differences were kept just for cells cultured for 5 and 10 days because the discrepancy disappeared with cells cultured for 15 days when compared to groups 2B, 3A and 3B. Interestingly, cells cultured for 10 and 15 days on constructs mineralized for 96 h in OST media (Group 4B) showed a higher cell number than its counterpart cultured in DMEM (Group 4A). The slight attenuation in the proliferation rates of cells cultured on mineralized SIS membranes compared to those cultured on non-mineralized SIS membranes (Fig. 6) could be explained by the fact that cells cultured on mineralized SIS membranes had a better osteogenic differentiation potential than non-mineralized SIS membranes as shown in next section (Fig. 7). It has been found that when cells started to differentiate very early, they would proliferate at a lower rate.<sup>50,51</sup> Differentiation of MSCs towards the osteoblastic lineage includes several steps. First, when seeded in osteogenic medium, cells have a high proliferation potential and start to proliferate and deposit ECM. Then cells exhibit a decreased proliferation rate and start to express characteristic bone proteins such as ALP. After this step, no major proliferation will be observed and a mature ECM will be formed with calcium deposition.<sup>52</sup>

### **Osteogenic Differentiation of MSCs on SIS Membranes**

ALP as an enzyme is an early marker for the osteogenic differentiation of MSCs.<sup>45,46</sup> The ALP activity was measured and normalized to the cell number of the respective sample (Fig. 7). The ALP assay showed an obvious increase in the enzyme activity on the groups of cells cultured with osteogenic supplements (OST) in comparison to those without osteogenic

Author Manuscript

Author Manuscript

Author Manuscript

supplements (DMEM). The highest ALP activity was detected in the Group 2B, i.e., cells seeded on SIS membranes nucleated with HAP for 12 h and cultured in OST media, which showed significant differences compared to the other groups. Groups 3B and 4B, i.e., cells seeded on SIS-HAP constructs formed with a mineralization time of 24 h and 96 h, respectively, and cultured in OST media, showed the next level of ALP activity. These cells also showed significant differences compared to the control group ( $p < 0.05$ ). The control group of cells seeded on the non-mineralized SIS membranes and cultured in OST media showed a moderate ALP activity compared to the mineralized SIS membranes. Either a drop or a lack of progress in the ALP activity on day 15 was found in all groups of cells seeded on the mineralized SIS membranes. A measurable level of ALP activity was found from all cells seeded on SIS-HAP membranes but cultured without osteogenic supplements (DMEM). These findings are significant for cells cultured for 10 days in group 3A and for both 5 and 10 days in group 4A compared to controls. We also used real-time PCR assay to verify the gene expression of OCN, which is a marker for the late stage of the osteogenic differentiation of MSCs. Our result showed that the OCN gene expression level was the highest for the SIS membranes mineralized for 12 h in both OST and DMEM media (Fig. 8). This result indicates that mineralization for an adequate period of time is better for producing a material capable of promoting the osteogenic differentiation of MSCs, probably because there exists an optimal range of the content of the minerals for the SIS membranes to achieve the best osteogenic differentiation of MSCs. Overall, our data show that biomineralization of SIS membranes could induce the osteogenic differentiation of MSCs in DMEM without osteogenic supplements and further promote the osteogenic differentiation of MSCs in OST. These results are consistent with earlier findings that HAP could promote the osteogenic differentiation of MSCs and bone formation.<sup>31–35,49,53–55</sup>

### Histological Evaluation of MSC-Seeded HAP-SIS Membranes

Author Manuscript

Histological evaluation showed that cells deposited ECM and were embedded in newly deposited ECM, forming several layers of cells on the top of the SIS membrane covering the whole scaffold (Figs. 9 and 10). There were no histological differences between constructs containing cells on the SIS membranes and those on HAP-SIS membranes, suggesting that biomineralized SIS membranes have biocompatibility comparable to SIS alone. Some cells were found to migrate towards the nanofibrous porous structure of the membranes, which was particularly true for the SIS membranes with 96 h of nucleation (Fig. 9), probably because biomineralization for 96 h showed increased cell attachment to the scaffolds (Fig. 4). This result indicates that biomineralization of the SIS membranes can promote the integration between new tissue and the scaffolds for enhanced *in vivo* bone regeneration.

## DISCUSSION

Author Manuscript

The aim of this study was to evaluate the *in vitro* performance of HAP-SIS membranes in directing the attachment, proliferation and differentiation of MSCs towards the osteoblastic lineage. For this purpose, MSCs were seeded on the mineralized SIS membranes and cultured for 5, 10 and 15 days in either MEM or OST media (i.e., media supplemented with dexamethasone, ascorbic acid and  $\beta$ -glycerophosphate). This preliminary study demonstrates



the feasibility of culturing and differentiating bone marrow MSCs toward the osteoblastic lineage on the the biomaterialized SIS scaffolds.

An ideal material for bone regeneration must comply with several characteristics: (1) biocompatible; (2) available in nature; (3) adapting to the natural tissue environment; (4) non-immunogenic; (5) biodegradable on a predictable time lapse; and (6) osteoinductive and osteoconductive. SIS membranes satisfy most of these premises.<sup>14-19</sup> Their high collagen content makes it mimic the compositions of bones, particularly after biomaterialization to form HAP. They can be retrieved very easily from natural tissues and biocompatibility studies report a mild inflammatory reaction from their implantation in the body.<sup>14-19</sup> Our study confirms that SIS membranes with and without mineralization are biocompatible. It further indicates that the biomaterialization of the SIS membranes promotes the attachment, growth and osteogenic differentiation of MSCs as well as the migration of cells into the scaffolds, and thus will make the SIS membranes more osteoinductive and osteoconductive.

Mineralized type I collagen fibrils are the basic building block of natural bone's structure and the mineralization of collagen confers the strength to support other structures in the body. By mimicking the basic structure of normal bone, biomaterialization of scaffolds could increase the osteoinductive and osteoconductive potential of the materials for tissue engineering applications.<sup>56</sup> In the present study, the XRD and SEM data show that HAP crystals are aligned along the collagen fibers, mimicking the structure of natural bone ECM. It has been described that the method used to mineralize the scaffolds plays a critical role in the mineralization process of materials.<sup>57</sup> In our approach, we have used a HAP-supersaturated solution to gradually mineralize the SIS membranes without the overwhelming chemical process necessary for HAP synthesis from calcium and phosphate ions. On the other hand, the main component of the SIS membranes is type I collagen fibers, a natural biomaterial used in many tissue engineering applications and described as an important element in the mineralization and cell adhesion processes of bone.<sup>58</sup> Therefore, the HAP-SIS scaffolds mimic the bone ECM and are expected to promote the bone formation.

Demonstrating a biomaterialized ECM (i.e., calcium deposition test) has been suggested as an indicator for the osteogenic capacity of a material *in vitro*.<sup>59,60</sup> However, our biomaterialized SIS membranes already contain bone minerals prior to cell seeding. Hence, we detected the formation of two osteogenic makers (ALP for early stage differentiation and OCN for late stage differentiation) and verified the differentiation of MSCs towards the osteoblastic lineage since the formation of these biomarkers indicated the commitment of MSCs to become osteoblasts.<sup>44</sup> In our study, the ALP activity measurements showed an intense differentiation process towards the osteoblastic lineage. ALP activity was detected early (day 5) in this study (Fig. 7) and showed the typical pattern described in the literature.<sup>50,52</sup> OCN gene expression profiling by real-time PCR assay also showed that the biomaterialization of SIS membranes for a suitable period of time would induce the osteogenic differentiation of MSCs in DMEM (Fig. 8). Namely, our study discovered that HAP-SIS membranes could induce the differentiation of MSCs in basal DMEM media without osteogenic factors. This finding is in accordance with the previous discovery that HAP by itself promoted MSC differentiation.<sup>35</sup> This finding is a plus in using HAP-SIS

membranes for guided bone regeneration since it shows an enhancement of the osteoconductive capabilities of the constructs.

## CONCLUSIONS

HAP crystals can be nucleated on the SIS membranes from a HAP-supersaturated solution to form biocompatible biomineralized scaffolds where HAP crystals are coated on the surface of collagen fibers constituting the membranes. The resultant HAP-SIS membranes show a good performance for supporting the attachment, proliferation and differentiation of MSCs toward the osteoblastic lineage. More importantly, the biomineralized SIS membranes can induce osteogenic differentiation of MSCs in DMEM without osteogenic supplements due to the presence of bone minerals. These results are predictable since the components found in these constructs are mainly made of type I collagen fibers, hydroxyapatite and some growth factors, all found in natural bones. These results suggest that it is possible to form biomineralized SIS membranes to build constructs for applications in bone regeneration.

## Acknowledgments

We would like to thank the financial support from National Science Foundation (CBET-0854465, CMMI-1234957, CBET-0854414, and DMR-0847758), National Institutes of Health (HL0925264, EB015190, AR056848), Department of Defense Peer Reviewed Medical Research Program (W81XWH-12-1-0384), Oklahoma Center for the Advancement of Science and Technology (HR11-006) and Oklahoma Center for Adult Stem Cell Research (434003). MY also thank the generous support from National High Technology Research and Development Program 863 (2013AA102507), Zhejiang Provincial Natural Science Foundation of China (LZ12C17001), National Natural Science Foundation of China (20804037 and 21172194) and Silkworm Industry Science and Technology Innovation Team (2011R50028).

## References

1. Salgado AJ, Coutinho OP, Reis RL. Bone tissue engineering: State of the art and future trends. *Macromol Biosci.* 2004; 4:743. [PubMed: 15468269]
2. Hing KA. Bone repair in the twenty-first century biology, chemistry or engineering? *Phil Trans R Soc Lond A.* 2004; 362:2821.
3. Green D, Walsh D, Mann S, Oreffo RO. The potential of biomimetics in bone tissue engineering: Lessons from the design and synthesis of invertebrate skeletons. *Bone.* 2002; 30:810. [PubMed: 12052446]
4. Murphy WL, Mooney DJ. Molecular-scale biomimicry. *Nat Biotechnol.* 2000; 20:30. [PubMed: 11753357]
5. Griffith LG, Naughton G. Tissue engineering: Current challenges and expanding opportunities. *Science.* 2002; 295:1009. [PubMed: 11834815]
6. Hartgerink JD, Beniash E, Stupp SI. Self-assembly and mineralization of peptide-amphiphile nanofibers. *Science.* 2001; 294:1684. [PubMed: 11721046]
7. Venugopal J, Giri Dev VR, Senthilram T, Ramakrishna S. Osteoblast mineralization with composite nanofibrous substrate for bone tissue regeneration. *Cell Biol Int.* 2011; 35:73. [PubMed: 20923413]
8. Suganya S, Venugopal J, Lakshmi B, Ramakrishna S, Giri Dev VR. Aloe vera/silk fibroin/hydroxyapatite incorporated electrospun nanofibrous scaffold for enhanced osteogenesis. *J Biomater Appl.* 2014; 4:9.
9. Wang J, Yang M, Zhu Y, Wang L, Tomsia AP, Mao CB. Phage nanofibers induce vascularized osteogenesis in 3D printed bone scaffolds. *Adv Mater.* 2014; 10.1002/adma.201400154
10. Weiner S, Wagner HD. The material bone: Structure-mechanical function relations. *Annu Rev Mater Sci.* 1998; 28:271.

11. Mann, S. *Biomaterialization: Principles and concepts in bioinorganic materials chemistry*. Oxford University Press; New York: 2001. p. 1
12. Du C, Falini G, Fermani S, Abbott C, Moradian-Oldak J. Supramolecular assembly of amelogenin nanospheres into birefringent microribbons. *Science*. 2005; 307:1450. [PubMed: 15746422]
13. Sato M, Webster TJ. Nanobiotechnology: Implications for the future of nanotechnology in orthopedic applications. *Expert Rev Med Devices*. 2004; 1:105. [PubMed: 16293014]
14. Badylak SF, Record R, Lindberg K, Hodde J, Park K. Small intestinal submucosa: A substrate for *in vitro* cell growth. *J Biomater Sci*. 1998; 9:863.
15. Voytik-Harbin SL, Brightman AO, Kraine MR, Waisner B, Badylak SF. Identification of extractable growth factors from small intestinal submucosa. *J Cell Biochem*. 1997; 67:478. [PubMed: 9383707]
16. Kropp BP, Ludlow JK, Spicer D, Rippey MK, Badylak SF, Adams MC, Keating MA, Rink RC, Birhle R, Thor KB. Rabbit urethral regeneration using small intestinal submucosa onlay grafts. *Urology*. 1998; 52:138. [PubMed: 9671888]
17. Badylak SF, Kropp B, McPherson T, Liang H, Snyder PW. Small intestinal submucosa: A rapidly resorbed bioscaffold for augmentation cystoplasty in a dog model. *Tissue Eng*. 1998; 4:379. [PubMed: 9916170]
18. Caione P, Capozza N, Zavaglia D, Palombaro G, Boldrini R. *In vivo* bladder regeneration using small intestinal submucosa: Experimental study. *Pediatr Surg Int*. 2006; 22:593. [PubMed: 16773371]
19. Ayyildiz A, Akgul KT, Huri E, Nuhoglu B, Kilicoglu B, Ustun H, Gurdal M, Germiyanoglu C. Use of porcine small intestinal submucosa in bladder augmentation in rabbit: Long-term histological outcome. *ANZ J Surg*. 2008; 78:82. [PubMed: 18199213]
20. Clarke KM, Lantz GC, Salisbury SK, Badylak SF, Hiles MC, Voytik SL. Intestine submucosa and polypropylene mesh for abdominal wall repair in dogs. *J Surg Res*. 1996; 60:107. [PubMed: 8592400]
21. Lai JY, Chang PY, Lin JN. Body wall repair using small intestinal submucosa seeded with cells. *J Surg Res*. 2003; 38:1752.
22. Helton WS, Fisichella PM, Berger R, Horgan S, Espat NJ, Abcarian H. Short-term outcomes with small intestinal submucosa for ventral abdominal hernia. *Arch Surg*. 2005; 140:549. [PubMed: 15967902]
23. Chen MK, Badylak SF. Small bowel tissue engineering using small intestinal submucosa as a scaffold. *J Surg Res*. 2001; 99:352. [PubMed: 11469910]
24. Ledet EH, Carl AL, DiRisio DJ, Tymeson MP, Andersen LB, Sheehan CE, Kallakury B, Slivka M, Serhan H. A pilot study to evaluate the effectiveness of small intestinal submucosa used to repair spinal ligaments in the goat. *Spine J*. 2002; 2:188. [PubMed: 14589492]
25. Musahl V, Abramowitch SD, Gilbert TW, Tsuda E, Wang JH, Badylak SF, Woo SL. The use of porcine small intestinal submucosa to enhance the healing of the medial collateral ligament—a functional tissue engineering study in rabbits. *J Orthop Res*. 2004; 22:214. [PubMed: 14656683]
26. Gastel JA, Muirhead WR, Lifrak JT, Fadale PD, Hulstyn MJ, Labrador DP. Meniscal tissue regeneration using a collagenous biomaterial derived from porcine small intestine submucosa. *Arthroscopy*. 2001; 17:151. [PubMed: 11172244]
27. Badylak SF, Lantz GC, Coffey A, Geddes LA. Small intestinal submucosa as a large diameter vascular graft in the dog. *J Surg Res*. 1989; 47:74. [PubMed: 2739401]
28. Lantz GC, Badylak SF, Coffey AC, Geddes LA, Blevins WE. Small intestinal submucosa as a small-diameter arterial graft in the dog. *J Invest Surg*. 1990; 3:217. [PubMed: 2078544]
29. Lantz GC, Badylak SF, Hiles MC, Coffey AC, Geddes LA, Kokini K, Sandusky GE, Morff RJ. Small intestinal submucosa as a vascular graft: A review. *J Invest Surg*. 1993; 6:297. [PubMed: 8399001]
30. Raghavan D, Kropp BP, Lin HK, Zhang Y, Cowan R, Madihally SV. Physical characteristics of small intestinal submucosa scaffolds are location-dependent. *J Biomed Mater Res A*. 2005; 73:90. [PubMed: 15693016]

31. Lock J, Nguyen TY, Liu H. Nanophase hydroxyapatite and poly (lactide-co-glycolide) composites promote human mesenchymal stem cell adhesion and osteogenic differentiation *in vitro*. *J Mater Sci Mater Med*. 2012; 23:2543. [PubMed: 22772475]
32. Chou YF, Dunn JC, Wu BM. *J Biomed Mater Res B*. 2005; 75:81.
33. Bourgeois B, Laboux O, Obadia L, Gauthier O, Betti E, Aguado E. *J Biomed Mater Res B*. 2003; 65:402.
34. Rosa AL, Beloti MM, Van Noort R, Hatton PV, Devlin AJ. *Pesqui Odontol Bras*. 2002; 16:209. [PubMed: 12386681]
35. Ramires PA, Romito A, Cosentino F, Milella E. The influence of titania/hydroxyapatite composite coatings on *in vitro* osteoblasts behaviour. *Biomaterials*. 2001; 22:1467. [PubMed: 11374445]
36. Silverstone LM, Wefel JS, Zimmerman BF, Clarkson BH, Featherstone MJ. Remineralization of natural and artificial lesions in human dental enamel *in vitro*. Effect of calcium concentration of the calcifying fluid. *Caries Res*. 1981; 15:138. [PubMed: 6937261]
37. Mao CB, Li H, Cui F, Feng Q, Ma C. Oriented growth of phosphates on polycrystalline titanium in a process mimicking biomineralization. *J Crystal Growth*. 1999; 206:308.
38. Mao CB, Li H, Cui F, QF, Ma C. The functionalization of titanium with EDTA to induce biomimetic mineralization of hydroxyapatite. *J Mater Chem*. 1999; 9:2573.
39. Mao CB, Li H, Cui F, Feng Q, Wang H, Ma C. Oriented growth of hydroxyapatite on (0001) textured titanium with functionalized self-assembled silane monolayer as template. *J Mater Chem*. 1998; 8:2795.
40. Xu H, Cao B, George A, Mao CB. Self-assembly and mineralization of genetically modifiable biological nanofibers driven by beta-structure formation. *Biomacromolecules*. 2011; 12:2193. [PubMed: 21520924]
41. Cao, B.; Mao, CB. Chapter 10: Phage as a template to grow bone mineral nanocrystals. Virus hybrids as nanomaterials. In: Ratna, B.; Lin, B., editors. *Methods in Molecular Biology*. Vol. 1108. Humana Press; USA: 2014. p. 123-135.
42. Li D, Qu X, Newton SMC, Klebba PE, Mao CB. Morphology-controlled synthesis of silica nanotubes through pH-and sequence-responsive morphological change of bacterial flagellar biotemplates. *J Mater Chem*. 2012; 22:15702. [PubMed: 22865955]
43. Cao B, Mao CB. Oriented nucleation of hydroxylapatite crystals on spider dragline silks. *Langmuir*. 2007; 23:10701. [PubMed: 17850102]
44. Zhu H, Cao B, Zhen Z, Laxmi A, Li D, Liu S, Mao CB. Controlled growth and differentiation of mesenchymal stem cells on grooved films assembled from monodisperse biological nanofibers with genetically tunable surface chemistries. *Biomaterials*. 2011; 32:4744. [PubMed: 21507480]
45. Shi S, Gronthos S, Chen S, Reddi A, Counter CM, Robey PG, Wang C-Y. Bone formation by human postnatal bone marrow stromal stem cells is enhanced by telomerase expression. *Nature Biotechnol*. 2002; 20:587. [PubMed: 12042862]
46. Bera S, Seb GTK, Hasirci V. Bone tissue engineering on patterned collagen films: An *in vitro* study. *Biomaterials*. 2005; 26:1997.
47. Datta N, Holtorf HL, Sikavitsas VI, Jansen JA, Mikos AG. Effect of bone extracellular matrix synthesized *in vitro* on the osteoblastic differentiation of marrow stromal cells. *Biomaterials*. 2005; 26:971. [PubMed: 15369685]
48. Wang J, Wang L, Li X, Mao CB. Virus activated artificial ECM induces the osteogenic differentiation of mesenchymal stem cells without osteogenic supplements. *Sci Rep*. 2013; 3:1242. [PubMed: 23393624]
49. Yang M, Shuai Y, Zhang C, Chen Y, Zhu L, Mao CB, Yang HO. Biomimetic nucleation of hydroxyapatite crystals mediated by *Antheraea pernyi* silk sericin promotes osteogenic differentiation of human bone marrow derived mesenchymal stem cells. *Biomacromolecules*. 2014; 15:1185. [PubMed: 24666022]
50. Castano-Izquierdo H, Alvarez-Barreto J, van den Dolder J, Jansen JA, Mikos AG, Sikavitsas VI. Pre-culture period of mesenchymal stem cells in osteogenic media influences their *in vivo* bone forming potential. *J Biomed Mater Res A*. 2007; 82:129. [PubMed: 17269144]
51. Bruder SP, Fink DJ, Caplan AI. Mesenchymal stem cells in bone development, bone repair, and skeletal regeneration therapy. *J Cell Biochem*. 1994; 56:283. [PubMed: 7876320]

52. Lian JB, Stein GS. Concepts of osteoblast growth and differentiation: Basis for modulation of bone cell development and tissue formation. *Crit Rev Oral Biol Med*. 1992; 3:269. [PubMed: 1571474]
53. Ravichandran R, Venugopal J, Mukherjee S, Ramakrishna S. Precipitation of nanohydroxyapatite on PLLA/PBLG/Collagen nanofibrous structures for the differentiation of adipose derived stem cells to osteogenic lineage. *Biomaterials*. 2012; 33:846. [PubMed: 22048006]
54. Venugopal J, Rajeswari R, Shayanti M, Ramakrishna S. Electrospayed hydroxyapatite on polymer nanofibers to differentiate mesenchymal stem cells to osteogenesis. *J Biomater Sci Polym Ed*. 2013; 24:170. [PubMed: 22370175]
55. Zhang YZ, Venugopal JR, Ramakrishna S, Lim CT. Enhanced biomineralization of osteoblasts on a novel electrospun biocomposite nanofibrous scaffold of hydroxyapatite/collagen/ chitosan. *Tissue Eng A*. 2010; 16:1949.
56. Kretlow JD, Mikos AG. Review: Mineralization of synthetic polymer scaffolds for bone tissue engineering. *Tissue Eng*. 2007; 13:927. [PubMed: 17430090]
57. Tanahashi M, Matsuda T. Surface functional group dependence on apatite formation on self-assembled monolayers in a simulated body fluid. *J Biomed Mater Res*. 1997; 34:305. [PubMed: 9086400]
58. Thorwarth M, Schultze-Mosgau S, Wehrhan F, Kessler P, Srour S, Wiltfang J, Schlegel KA. Bioactivation of an anorganic bone matrix by P-15 peptide for the promotion of early bone formation. *Biomaterials*. 2005; 26:5648. [PubMed: 15878370]
59. Declercq HA, Verbeeck RM, De Ridder LI, Schacht EH, Cornelissen MJ. Calcification as an indicator of osteoinductive capacity of biomaterials in osteoblastic cell cultures. *Biomaterials*. 2005; 26:4964. [PubMed: 15769532]
60. Wang J, Yang Q, Mao CB, Zhang S. Osteogenic differentiation of bone marrow mesenchymal stem cells on the collagen/silk fibroin bi-template-induced biomimetic bone substitutes. *J Biomed Mater Res A*. 2012; 100:2929. [PubMed: 22700033]

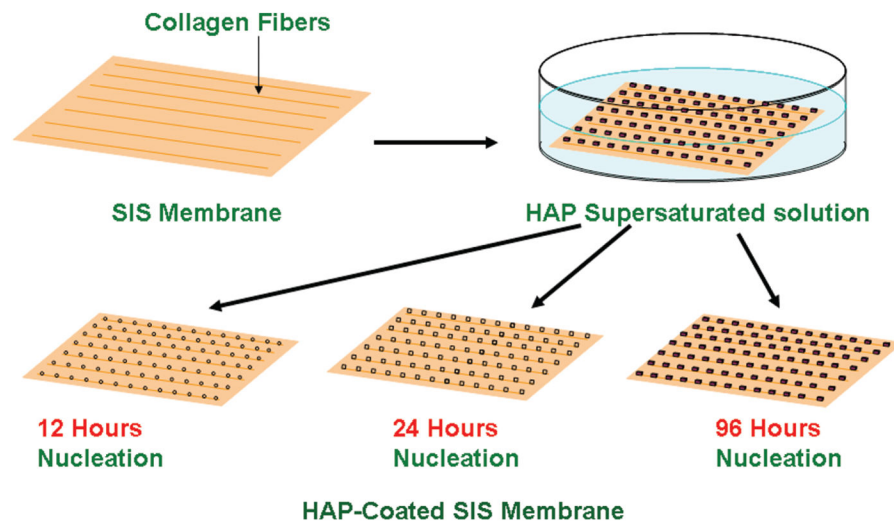


**Figure 1.** Schematic illustration of the biomimetic mineralization of the SIS membranes. The SIS membranes were placed into a HAP-supersaturated solution to induce the biomimetic mineralization for 12, 24, and 96 h.

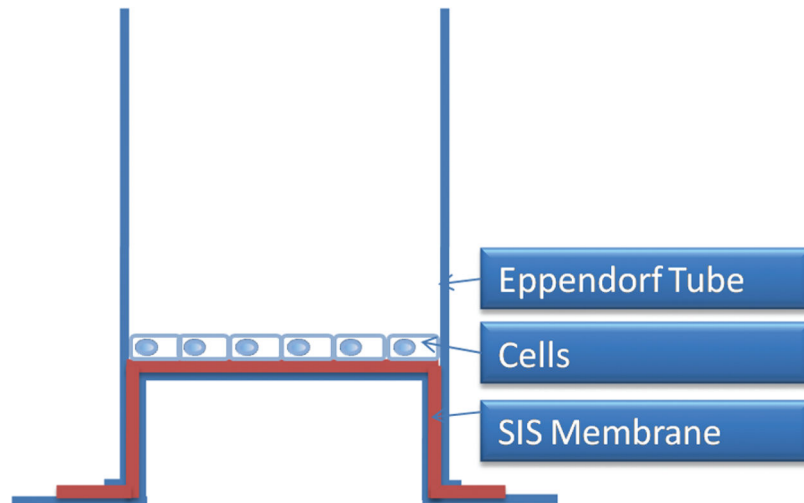


**Figure 2.** Schematic showing the arrangement of the small intestinal submucosa (SIS) membrane (mineralized or non-mineralized) on the Eppendorf tube and cells seeded on SIS membrane. This setup shows how the cells are cultured to evaluate the performance of SIS membranes in directing the attachment, proliferation and osteogenic differentiation of MSCs.

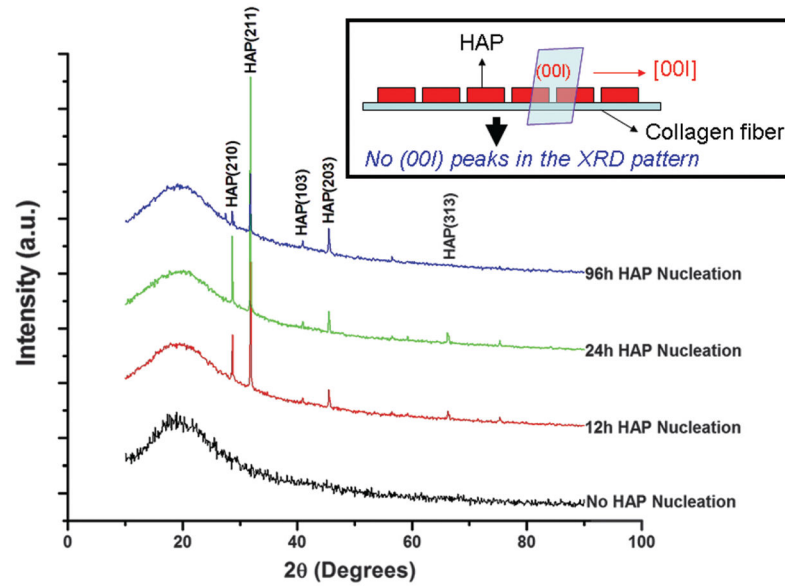


**Figure 3.** XRD patterns of SIS membranes mineralized for 0, 12, 24 and 96 h. The inset schematically illustrates that when HAP has  $c$ -axis preferred orientation along the collagen fibers lying on the SIS membrane, the  $(00l)$  peaks will be absent in the XRD patterns, which is the actual case in the XRD patterns shown here.



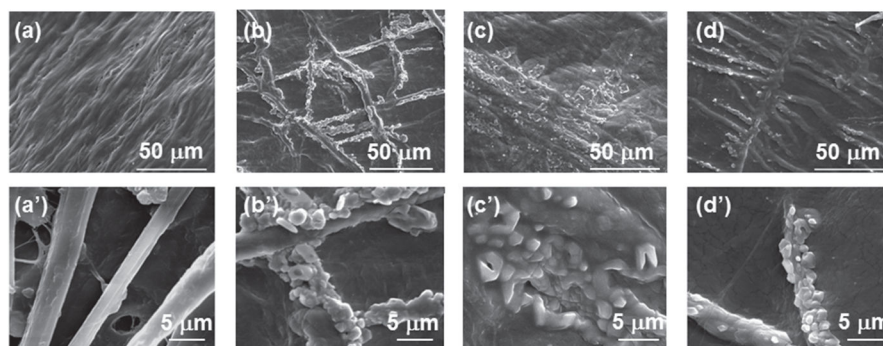


**Figure 4.** SEM images of SIS membranes after different mineralization times (0, 12, 24 and 96 h). (a)–(d) are typical images of the SIS membranes that were mineralized for 0, 12, 24 and 96 h, respectively. (a')–(d') are typical high magnification images taken from some areas on the the same membranes shown in (a)–(d), respectively.

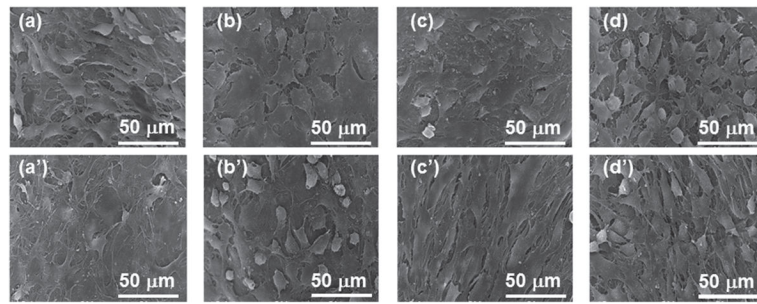


**Figure 5.** SEM images of cells attached onto the SIS membranes that were mineralized for 0 h ((a), (a')), 12 h ((b), (b')), 24 h ((c), (c')) and 96 h ((d), (d')). Top (a)–(d): cells on the scaffolds were cultured in the osteogenic media (OST). Bottom ((a)'–(d)'): cells on the scaffolds were cultured in DMEM.

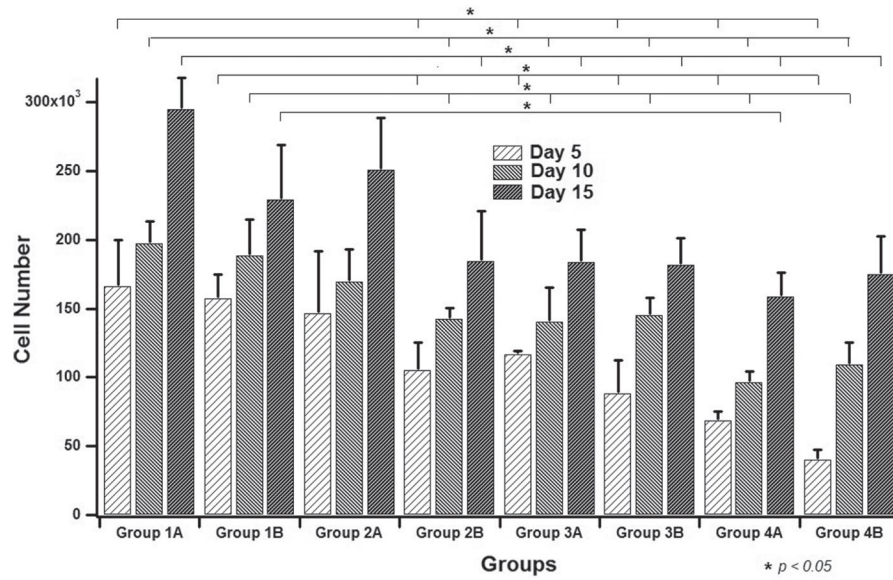


**Figure 6.** Cell number determined from DNA assay (by using PicoGreen dye) from all of the samples shown in Table I. Group 1: cells on non-mineralized SIS membranes; Group 2: cells on SIS membranes mineralized for 12 h; Group 3: cells on SIS membranes mineralized for 24 h; Group 4: cells on SIS membranes mineralized for 96 h. A: cultured in DMEM media; B: cultured in OST media.

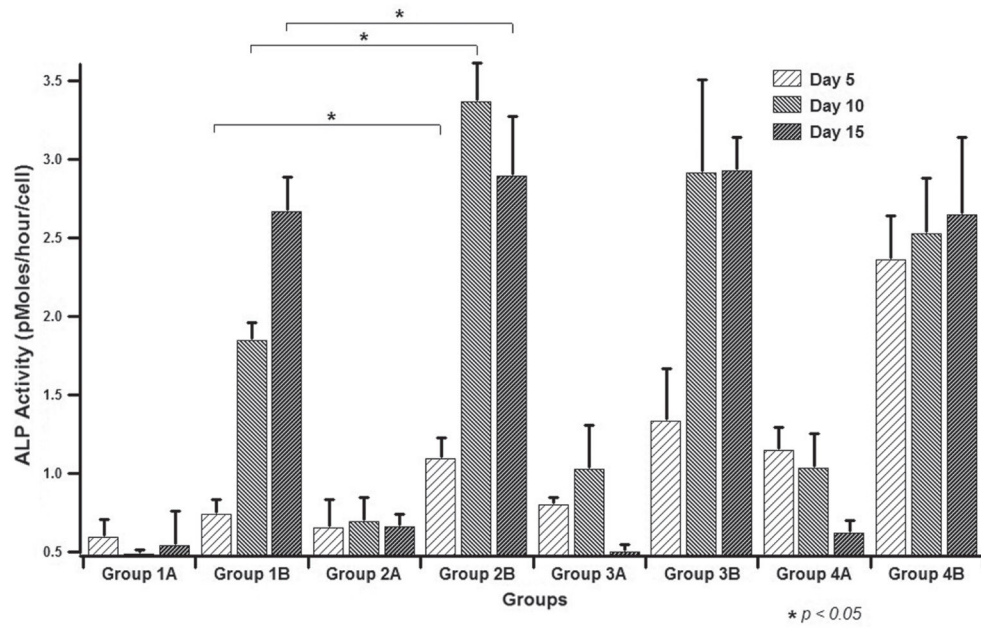


**Figure 7.** ALP assay results from all of the samples shown in Table I. Group 1: cells on non-mineralized SIS membranes; Group 2: cells on SIS membranes mineralized for 12 h; Group 3: cells on SIS membranes mineralized for 24 h; Group 4: cells on SIS membranes mineralized for 96 h. A: cultured in DMEM media; B: cultured in OST media.

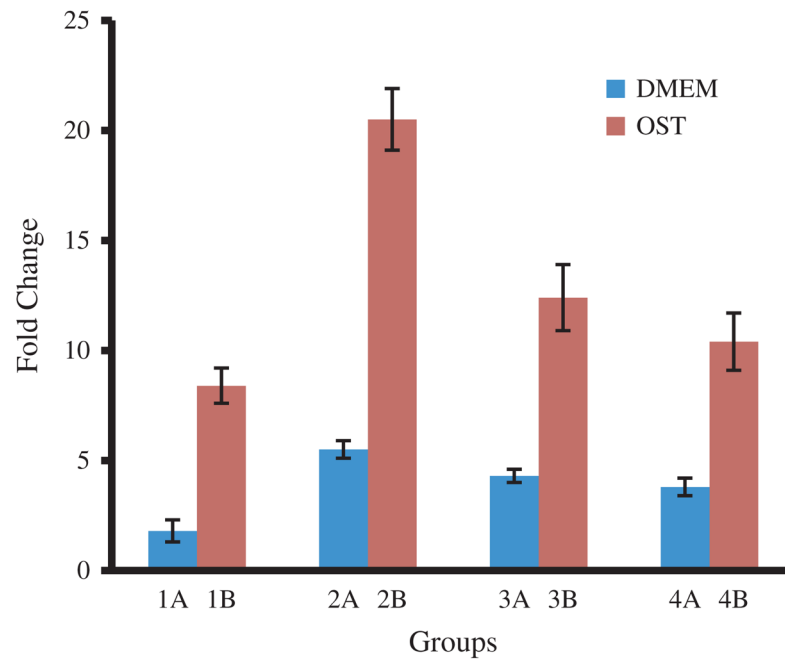


**Figure 8.**

Real-time PCR analysis showing the level of osteocalcin gene expression of cells cultured on different substrates in DMEM (Group A) and OST (Group B) media for 15 days. Group 1: non-mineralized SIS membranes; Group 2: SIS membranes mineralized for 12 h; Group 3: SIS membranes mineralized for 24 h; Group 4: SIS membranes mineralized for 96 h.

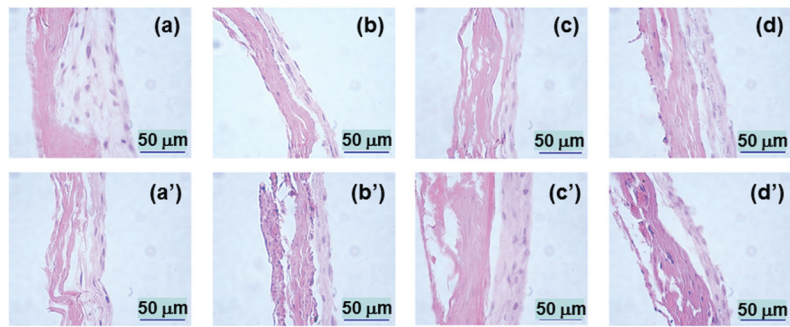


**Figure 9.** Histological images of the SIS membranes mineralized for 0 h ((a), (a')), 12 h ((b), (b')), 24 h ((c), (c')) and 96 h ((d), (d')) after MSCs were cultured on the membranes for 15 days. Top (a–d): images from scaffolds with cells cultured in OST. Bottom ((a')–(d')): images from scaffolds with cells cultured in DMEM. The explanation of the image is shown in Figure 10.

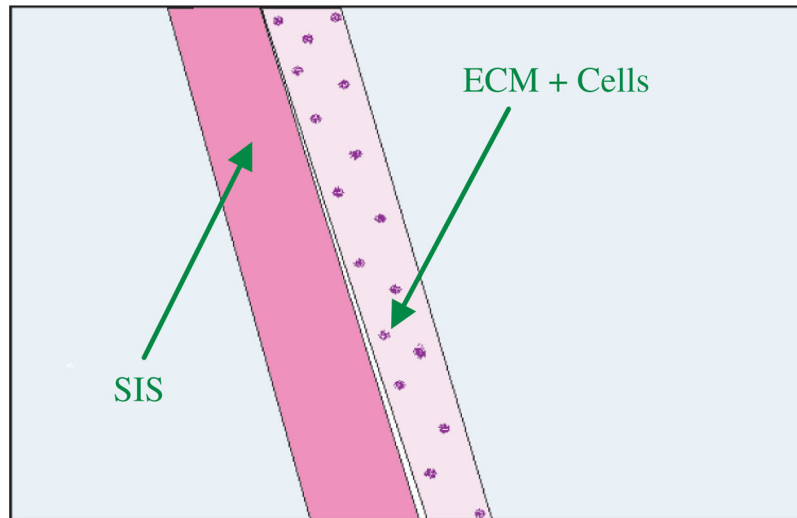


**Figure 10.** Schematic illustration of the histological images shown in Figure 9. The left side is the SIS membrane and the right side contains the cells and newly secreted ECM. Some cells migrated into the SIS membranes in Figure 9.

**Table I**

Experimental design based on mineralization time and cell culture media.

MSCs culture media	Groups/mineralization time (hours)			
	Group 1/0 h	Group 2/12 h	Group 3/24 h	Group 4/96 h
DMEM (A)	Culture time: 5, 10, 15 days	Culture time: 5, 10, 15 days	Culture time: 5, 10, 15 days	Culture time: 5, 10, 15 days
OST (B)	Culture time: 5, 10, 15 days	Culture time: 5, 10, 15 days	Culture time: 5, 10, 15 days	Culture time: 5, 10, 15 days

*Notes:* DMEM: Dulbecco's minimal essential media; OST: Osteogenic Media, made of DMEM supplemented with dexamethasone, ascorbic acid, and  $\beta$ -glycerophosphate.

Author Manuscript

Author Manuscript

Author Manuscript

Author Manuscript